

# The Molecularly Controlled Semiconductor Resistor: How does it work?

Eyal Capua,<sup>†</sup> Amir Natan,<sup>‡</sup> Leeor Kronik,<sup>‡</sup> and Ron Naaman<sup>\*·†</sup>

Department of Chemical Physics and Department of Materials and Interfaces, Weizmann Institute of Science, Rehovoth 76100, Israel

**ABSTRACT** We examine the current response of molecularly controlled semiconductor devices to the presence of weakly interacting analytes. We evaluate the response of two types of devices, a silicon oxide coated silicon device and a GaAs/AlGaAs device, both coated with aliphatic chains and exposed to the same set of analytes. By comparing the device electrical response with contact potential difference and surface photovoltage measurements, we show that there are two mechanisms that may affect the underlying substrate, namely, formation of layers with a net dipolar moment and molecular interaction with surface states. We find that whereas the Si device response is mostly correlated to the analyte dipole, the GaAs device response is mostly correlated to interactions with surface states. Existence of a silicon oxide layer, whether native on the Si or deliberately grown on the GaAs, eliminates analyte interaction with the surface states.

**KEYWORDS:** monolayer • molecularly controlled resistor • surface states • band bending • dipole layer

## I. INTRODUCTION

Controlling the properties of semiconductor devices and low-dimensional structures by means of a (full or partial) molecular layer is an important strategy for chemical sensing (1–6). This approach combines desired molecular properties, notably chemical specificity and design flexibility, with desired semiconductor device properties, notably controlled electrical conductivity and high sensitivity. One well-established example of this combination is the chemically sensitive field effect transistor (7–10). In this device, the presence of molecules influences the potential of the conducting field effect transistor (FET) channel, either by directly influencing the gate potential or by changing the potential distribution between a “reference electrode gate” and the semiconductor.

Some ten years ago, a different sensing technique was introduced, which we call the molecularly controlled semiconductor resistor (MOCSE) (11). In this approach, the traditional gating electrode is replaced by a molecular layer adsorbed directly on the semiconductor or on a typically very thin dielectric (with a back-gate electrode present in some cases). Interaction of the analyte with the molecular layer (or, in some case, the molecular layer itself *being* the analyte) changes the potential in the conducting channel. This modifies the current between source and drain, resulting in chemical sensing. Devices utilizing this principle have been demonstrated by many groups to sense a wide range of chemical and biochemical analytes, in gas phase and in liquid phase, based on a variety of molecular layers and (inorganic and organic) semiconducting substrates (12–20).

Generally speaking, it has often been assumed that such devices are sensitive to the dipole moment of the adsorbed species (11–13). Indeed, a linear correlation between the device response and the molecular dipole has been observed experimentally in some cases (14, 19). But this simple picture is not complete, for several reasons. Natan et al. (21) have shown theoretically that adsorption of an ideally ordered polar monolayer would typically result in a negligibly small device response due to a rapid decay of the electric fields outside the polar layer. Hence device response to the molecular dipole must depend on the degree of molecular (dis-)order. Cohen et al. (22) have shown experimentally that adsorption of molecules possessing the same binding group but different polar groups may significantly change the surface band bending by modifying the surface state distribution. Quite generally, then, molecular adsorption processes may change both the surface dipole and the surface band bending in subtle ways (23). Indeed, Shaya et al. have recently shown that both effects should be considered explicitly in their analysis of the signal observed at a silicon-based device (24) and that there certainly are conditions at which surface band bending changes dominate (25).

The above considerations imply that the sensitivity of the current through the semiconductor device to the analyte can be a strong function of the properties of the semiconductor, its surface, and the “sensing” molecular layer (26). However, to the best of our knowledge, no attempt has been made to characterize how different semiconductors are affected by the same set of analytes and whether different mechanisms dominate under different conditions. Here, we explore this issue by comparing two types of devices, a silicon oxide coated silicon device and a GaAs/AlGaAs device, both coated with aliphatic chains and exposed to the same set of analytes. By comparing the device electrical response with contact potential difference and surface photovoltage mea-

<sup>†</sup> Department of Chemical Physics.

<sup>‡</sup> Department of Materials and Interfaces.

Received for review August 23, 2009 and accepted October 25, 2009

DOI: 10.1021/am9005622

© 2009 American Chemical Society

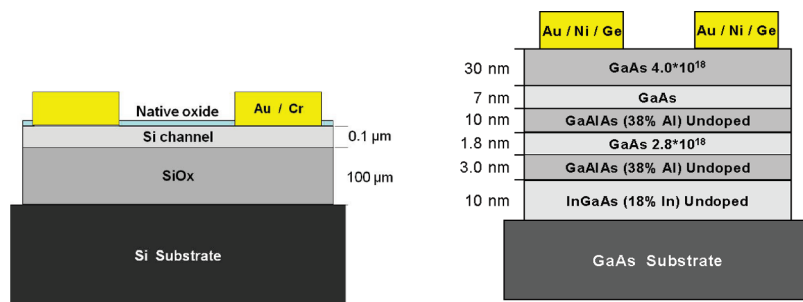


FIGURE 1. Schematic representation of the Si (left) and the GaAs/GaAlAs (right) based molecularly controlled semiconductor resistor devices used in this work. For the GaAs-based devices, interelectrode distances varying between 200 and 2000  $\mu\text{m}$  were examined, with the width of the conductive channel fixed at 200  $\mu\text{m}$ . In the silicon-based devices, the interelectrode distance was 5  $\mu\text{m}$  and the width of the channel was 750  $\mu\text{m}$ .

measurements (23), we find that whereas the Si device response is mostly correlated to the analyte dipole, the GaAs device response is mostly correlated to interactions with surface states.

## II. MATERIALS AND METHODS

**Device Fabrication and Electrical Measurements.** A schematic representation of the two basic structures used in this work is given in Figure 1. One device is based on silicon, whereas the other is based on GaAs/AlGaAs. The silicon-based device was fabricated by Intel Research Laboratories, Israel, with a conductive channel length and width of 5 and 750  $\mu\text{m}$ , respectively. The GaAs n-type pseudomorphic high electron mobility transistor devices were fabricated using photolithography in a standard clean-room, such that the conducting channel width was 200  $\mu\text{m}$  and its length varied from 200 to 2000  $\mu\text{m}$ . The electrical response of the devices to the various molecules does not depend on the channel length. All electrical measurements were performed with Keithley 236 source-measure units on wire bonded devices. GaAs devices were wired via the source and drain contact. Si devices were also biased via a back-gate contact.

**Molecular Modification.** Organic monolayers were adsorbed and characterized according to previously reported procedures (27, 28). Solvents were reagent grade or better, purchased from Merck, Baker, or Bio-Lab. 1-Octadecanephosphonate ( $\text{C}_{18}\text{Phosp}$ ) molecules were purchased from PCI Synthesis. Octyltrichlorosilane ( $\text{C}_8\text{Sil}$ ) molecules were purchased from Sigma-Aldrich. All chemicals were used without further purification. Monolayer quality was verified by ellipsometry (J. A. Woollam, model M-2000 V) measurements, within a range of 399–1000 nm, as well as by contact angle measurements.

GaAs devices were sonicated prior to molecular adsorption in isopropanol, acetone, and ethanol for 10 min each, followed by UV/ozone oxidation (UVOCS) for 10 min. The substrates were then etched for 5 s in 2% HF, rinsed in water, dipped for 30 s in  $\text{NH}_4\text{OH}$  (about 25%  $\text{NH}_3$ ), and rinsed in water again. After they were dried under an  $\text{N}_2$  stream, the samples were immediately placed in the adsorption solution.  $\text{C}_{18}\text{Phosp}$  monolayers were prepared from a 1 mM tetrahydrofuran (THF) adsorption solution. Adsorption was carried out overnight in  $\text{N}_2$ -filled vials placed in a desiccator. After adsorption, the samples were rinsed with THF and  $\text{N}_2$ -dried.

Si devices were sonicated prior to adsorption in ethyl acetate for 2 min, rinsed with acetone and ethanol, followed by UVOCS for 20 min. The devices were placed three times for 30 s in 1 mM  $\text{C}_8\text{Sil}$  in bicyclohexyl (BCH) adsorption solutions. After each dip, the samples were rinsed and sonicated for 30 s in toluene.

Importantly, in the Si-based devices molecular monolayers were adsorbed on top of a 2 nm thick, native silicon oxide layer,

whereas in the GaAs-based ones molecular monolayers were adsorbed directly on the GaAs surface after removal of the oxide layer.

**Analytes.** The analytes used in this work were acetone (Ace), 99.9% ethanol (EtOH), 99% benzonitrile (BZN), 30% hydrogen peroxide ( $\text{H}_2\text{O}_2$ ), and triacetone triperoxide (TATP). Ace, EtOH, and  $\text{H}_2\text{O}_2$  were purchased from J.T. Baker. BZN was purchased from Sigma-Aldrich. TATP was produced in-house with extreme caution.

Electric measurements of analyte-exposed devices were performed in a dark chamber with a constant flow of  $\text{N}_2$  that was set to a rate of 500 cc/min. The different analytes were evaporated in a 30 mL chamber at room temperature, and the vapors were carried by a constant  $\text{N}_2$  flow of 80 cc/min. This stream of nitrogen was combined with the main nitrogen flow and then introduced into the sensor chamber.

**Work Function and Band-Bending Measurements.** Contact potential difference (CPD) or surface photovoltage (SPV) measurements (23) were conducted on substrates identical to those used for device manufacturing that were modified molecularly and exposed to analyte molecules in the same manner described above. CPD measurements were performed using the Kelvin probe technique (23), with a vibrating gold grid acting as the reference (probe) electrode, using a Besocke Delta Phi commercial setup. The sample and the probe were placed in a closed metallic box, acting as a Faraday cage so as to avoid electrical interference from external sources. SPV measurements were conducted while measuring CPD by illuminating the sample with a 632 nm HeNe laser.

## III. RESULTS

The response of the Si/SiOx/ $\text{C}_8\text{Sil}$  and the GaAs/ $\text{C}_{18}\text{Phosp}$  based devices to the various analytes is given in Figure 2. In both devices the functional group exposed to the gas is obviously a methyl group. Interestingly, despite this similarity the response of the two devices to the different analytes is completely different and in fact almost complementary. The GaAs-based devices respond to TATP and  $\text{H}_2\text{O}_2$ , but do not respond to acetone or ethanol. Exactly the opposite is true for the Si-based devices. Of the analytes we studied, response from both types of devices was obtained only with BZN, but even then the sign of the response is different. Importantly, upon coating the GaAs-based device with a (thicker) silicon oxide layer, followed by coating with alkyl silane, as described above, the response of the GaAs-based device to the different analytes became qualitatively similar to that of the Si-based device (albeit smaller, because of the increased thickness of the oxide).

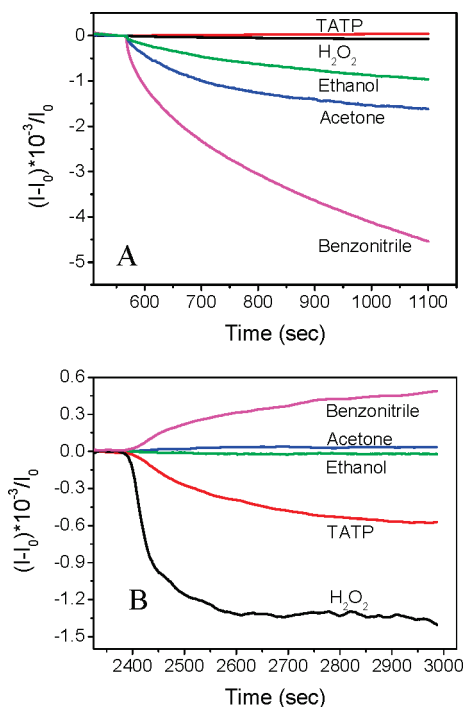


FIGURE 2. Normalized change in current as a function of time for Si/SiO<sub>x</sub> (A) and GaAs (B) based devices. Si and GaAs devices were covered with C<sub>8</sub>Sil and C<sub>18</sub>Phosp, respectively (see text for details). The devices were exposed to vapors of TATP (10 ppm), hydrogen peroxide (110 ppm), ethanol (1.5 × 10<sup>4</sup> ppm), acetone (6.1 × 10<sup>4</sup> ppm), and benzonitrile (130 ppm).

To assess the importance of the analyte dipole in determining the response of the Si-based devices we measured the CPD response of the Si/SiO<sub>x</sub>/C<sub>8</sub>Sil structure to the different analytes. The analyte-induced *change* in the device current, as a function of the analyte-induced CPD change, is given in Figure 3. A clear correlation ( $R = 0.98$ ) is found. Figure 3 also shows the dipole moment of the gas-phase analyte molecules (29). With the notable exception of H<sub>2</sub>O<sub>2</sub>, the device response also shows a significant correlation to the analyte dipole moment (though not as high as that found with the CPD). Unfortunately, for the GaAs-based devices the CPD readings were not stable enough to allow for a similar plot. However, it is clear that in this case the device response does not correlate at all with the analyte molecular dipole moment.

To assess the importance of surface state interactions in determining the device response, we measured the transient light-on and light-off SPV response of both Si- and GaAs-based devices, for the different analytes used (Figure 4). Illumination of the substrate causes band flattening and therefore in the case of band bending mechanism, one expects to observe a significant change in the CPD signal with and without the adsorbed analyte. In all cases, the superbandgap illumination results in a CPD decrease due to illumination-induced reduction in the semiconductor surface band-bending (23). However, whereas for the Si-based devices the SPV transients appear to be short and largely independent of the analyte, in the GaAs-based devices there is a distinct slow transient component upon illumination

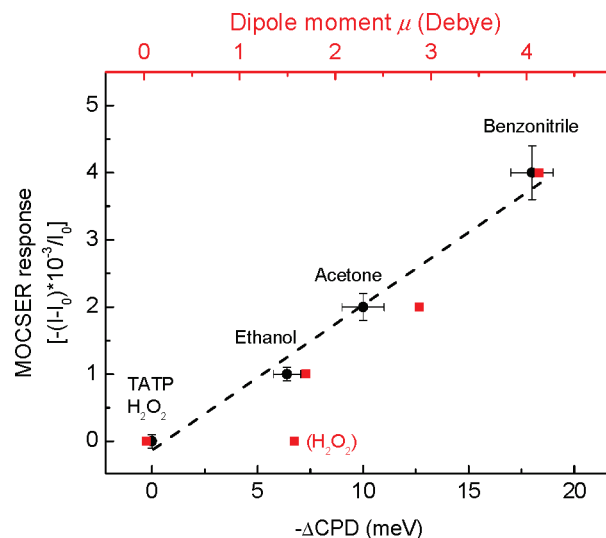


FIGURE 3. Correlation plot for Si-based MOCSESR response, CPD value, and molecular dipole, for the various analytes used. CPD measurements were carried out on slabs of n-type Si (<1 0 0>) possessing a native oxide and covered with a monolayer of C<sub>8</sub>Sil. Analyte exposure is the same as in Figure 2. The black dots indicate the MOCSESR response as a function of  $\Delta$ CPD, while the red squares indicate the relation between the MOCSESR responses and the respective molecular dipole moments. The dashed line represents the linear fit measured between the devices response and the correlated  $\Delta$ CPD, with a correlation factor of  $R = 0.98$ .

switch-off. This component is reduced significantly in the presence of TATP or H<sub>2</sub>O<sub>2</sub>.

#### IV. DISCUSSION

Naively, one would have expected the analyte molecules to elicit a qualitatively similar response from the Si- and GaAs-based molecularly controlled sensing devices, given that the analytes are nominally exposed to a similar chemical environment. However, Figure 2 establishes that this is definitely not the case.

The excellent correlation between CPD changes and device response in the Si-based device clearly suggests that in this case the device does respond to the net dipole of the formed overlayer. Furthermore, because all adsorbed analytes, to which the device responds, reduce the work function, we conclude that the positive pole of the net dipole generated by the analyte is pointing away from the surface.

The analyte-bearing monolayer is not a well-packed, highly organized layer. Therefore we do not expect a “dipolar layer” in the traditional sense of the term to form upon exposure to the analyte. As mentioned above, the electric field outside a close-packed, highly ordered monolayer decays exponentially as a function of distance from the layer, so that a device response would not be expected (21). Hence, it is the lack of perfect order and coverage that in principle allows for penetration of electric fields into the semiconductor region, resulting in device response. Sensitivity to the degree of coverage is further supported by the fact that the correlation with the analyte molecular dipole exists but is smaller than the correlation with the CPD changes. This is because the CPD reflects the *actual net* dipole formed, so that for perfect correlation with the molecular dipole to be preserved the degree of order (i.e., percent coverage,

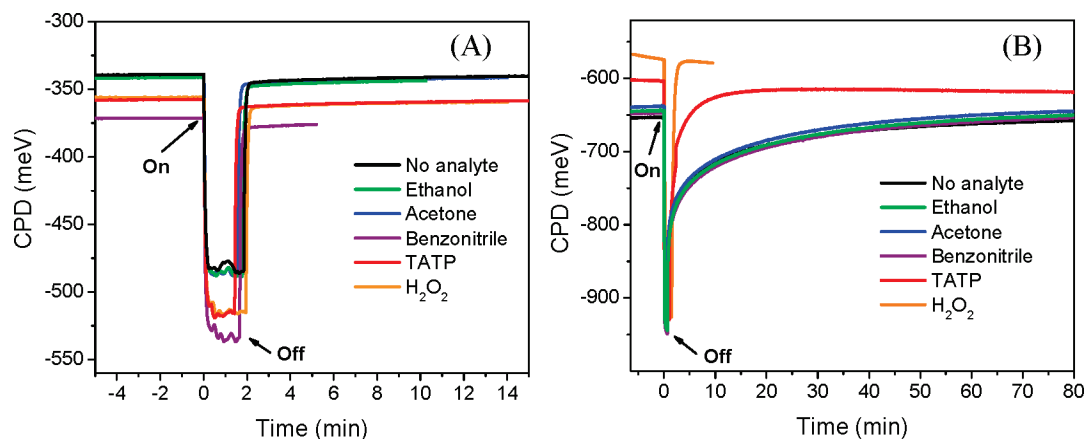


FIGURE 4. Surface photovoltage (SPV) measurement for Si (A) and GaAs (B) slabs covered with respective monolayers. Illumination was performed during analyte exposure at time zero for 2 min (note “On” and “Off” designations in the figures).

average orientation) would have to be the same throughout. Specifically, exposure to  $\text{H}_2\text{O}_2$  elicits neither CPD nor current response, even though the molecule does have a net dipole. This indicates that the  $\text{H}_2\text{O}_2$  is adsorbed with a completely random orientation, with its net dipole parallel to the surface, or not at all.

We note that lack of ideal order and coverage does not *guarantee* that an electric field large enough to result in a measurable device response will be present at the semiconductor, especially with an oxide layer (25). Nevertheless, the correlations observed between the molecular dipole and the response of the Si-based devices suggest that the appropriate conditions are present in this case. Furthermore, we did not find a correlation with other molecular properties that could in principle induce charge transfer processes, for example, their ionization potential or electron affinity.

Because in the GaAs-based devices correlation with the molecular dipole is absent, the physical mechanism at work is obviously different. A key observation is that the Si-based devices possess an oxide layer, whereas the GaAs-based devices do not. The presence of a significant slow component in the SPV relaxation transient generally implies the presence of deep surface states (23) and is typical to etched GaAs surfaces (30). Furthermore, it has been recently shown specifically that adsorption of alkylphosphonate monolayers on etched GaAs does not eliminate the surface band bending (31). We conclude, therefore, that the etched GaAs surface has not been fully passivated by the  $\text{C}_{18}\text{Phosp}$  overlayer. This makes the GaAs-based device much more susceptible to monopolar effects, where surface charge is removed upon molecule-surface interaction that eliminates the surface states (22). Indeed, except for BZN, device response is observed if and only if the slow transient indicative of surface states is noticeably diminished by the analyte. As mentioned in the preceding section, in the presence of a deliberately grown silicon oxide layer that is thick enough to mask the GaAs surface from the analyte, the GaAs-based device reverts to behaving like a Si-based one. We take this as conclusive evidence that the absence of oxide is indeed responsible for the large qualitative difference in GaAs-based device behavior.

Interestingly, the analyte-surface interaction occurs even though the surface is coated with a fairly well-organized monolayer consisting of 18-carbon-long alkyl chains. It is known that the density of surface states in bare GaAs surface is of the order of  $10^{15} \text{ cm}^{-2}$  (32), but that this number is reduced by a factor of  $\sim 20$  upon formation of the monolayer (33). Because a dense monolayer contains  $\sim 10^{14}$  molecules/ $\text{cm}^2$ , net transfer of a small fraction of charge, much less than 1% per molecule, is more than sufficient to affect an easily detectable change in the device (34). Indeed, we observed that the more organized and dense the self-assembled monolayer on top of the GaAs is, the higher the device sensitivity to the analytes is.

Of all the analytes studied, only BZN elicits a response from both Si- and GaAs-based devices, even though no interaction with the GaAs surface states is observed. We conclude that BZN is detected via its dipole in both cases, a conclusion consistent with the expected higher degree of order of a BZN layer as compared to the other analytes. Curiously, the response of Si- and GaAs-based devices is opposite in sign. Likely this reflects a significantly different adsorption configuration for the BZN overlayer, although it should be borne in mind that for sufficiently well-ordered overlayer, a close to complete coverage can result in an inverted sign of response (21).

Finally, why is it that adsorption of the same analytes on seemingly similar monolayers can be so different? We believe that while the local chemical environment is similar, the electrostatic landscape is different. Evidence for this can be found in the CPD. At equilibrium, for a sufficiently thick overlayer, the external surface is effectively decoupled from any internal interface and the CPD reflects the work function of the overlayer (23, 35). Alkane chains are insulating and possess low polarizability and therefore their external group is not screened from the semiconductor. Indeed, CPD values of the analyte-free Si/SiOx/ $\text{C}_8\text{Sil}$  and GaAs/ $\text{C}_{18}\text{Phosp}$  layers differ by  $\sim 300$  meV, well above any measurement error or instability. This indicates that despite the local similarity, the chemical environment the analyte “sees” in the two types of devices is *not* identical. Likely this different electrostatic environment, as reflected in the CPD difference, also ex-

plains the significant difference in orientation and/or coverage of the BZN molecules on the two surfaces.

## V. CONCLUSIONS

In this study, we examined the response of MOCSEER devices to analytes that do not interact strongly with the substrates, that is, interact via weak dispersive or high order electrostatic interactions. We compared the response of two types of devices, a silicon oxide coated silicon device and a GaAs/AlGaAs device, both coated with aliphatic chains and exposed to the same set of analytes. By comparing the device electrical response with contact potential difference and surface photovoltage measurements, we demonstrated that there are two mechanisms that may affect the underlying substrate: formation of layers with a net dipolar moment and molecular interaction with surface states. Because only a small fraction of charge is needed to affect the device, this second mechanism may well be operative even in cases that would not be typically characterized as “charge transfer” scenarios. Which mechanism dominates is a strong function of both substrate and analyte. In this case, we found that whereas the Si device response is mostly correlated to the analyte dipole, the GaAs device response is mostly correlated to interactions with surface states, and attributed this difference to the presence or absence, respectively, of a silicon oxide layer. This suggests that it should be possible to design adsorbed monolayers that will interact specifically and strongly with the analyte and will elicit a significant device response via one or both of the mechanisms suggested here.

**Acknowledgment.** We thank Dr. Ilan Levy (Intel Research Laboratories, Israel) for supplying silicon-based devices and the Israel Science Foundation for partial support of this work. R.N. and L.K. acknowledge the partial support of the Grand Center at the Weizmann Institute and the Lise Meitner-Minerva center for Computational Chemistry, respectively.

## REFERENCES AND NOTES

- (1) Seker, F.; Meeker, K.; Kuech, T. F.; Ellis, A. B. *Chem. Rev.* **2000**, *100*, 2505–2536.
- (2) (a) Cui, Y.; Wei, Q.; Park, H.; Lieber, C. M. *Science* **2001**, *293*, 1289–1292. (b) Cui, Y.; Lieber, C. M. *Science* **2001**, *291*, 851–853.
- (3) Ashkenasy, G.; Cahen, D.; Cohen, R.; Shanzer, A.; Vilan, A. *Acc. Chem. Res.* **2002**, *35*, 121–128.
- (4) Bent, S. F. *Surf. Sci.* **2002**, *500*, 879–903.
- (5) Mabeck, J. T.; Malliaras, G. G. *Anal. Bioanal. Chem.* **2006**, *384*, 343–353.
- (6) Somers, R. C.; Bawendi, M. G.; Nocera, D. G. *Chem. Soc. Rev.* **2007**, *36*, 579–591.
- (7) Bergveld, P. *Sens. Actuators B* **2003**, *88*, 1–20.
- (8) Janata, J. *Electroanalysis* **2004**, *16*, 1831–1835.
- (9) Schöning, M. J. *Sensors* **2005**, *5*, 126–138.
- (10) Albert, K. J.; Lewis, N. S.; Schauer, C. L.; Sotzing, G. A.; Stitzel, S. E.; Vaid, T. P.; Walt, D. R. *Chem. Rev.* **2000**, *100*, 2595–2626.
- (11) (a) Gartsman, K.; Cahen, D.; Kadyshevitch, A.; Libman, J.; Moav, T.; Naaman, R.; Shanzer, A.; Umansky, V.; Vilan, A. *Chem. Phys. Lett.* **1998**, *283*, 301–306. (b) Vilan, A.; Ussyshkin, R.; Gartsman, K.; Cahen, D.; Naaman, R.; Shanzer, A. *J. Phys. Chem. B* **1998**, *102*, 3307–3309.
- (12) Wu, D. G.; Cahen, D.; Graf, P.; Naaman, R.; Nitzan, A.; Shvarts, D. *Chem.—Eur. J.* **2001**, *7*, 1743–1749.
- (13) (a) Rudich, Y.; Benjamin, I.; Naaman, R.; Thomas, E.; Trakhtenberg, S.; Ussyshkin, R. *J. Phys. Chem. A* **2000**, *104*, 5238–5245. (b) Vilar, M. R.; El-Beghdadi, J.; Debontridder, F.; Naaman, R.; Arbel, A.; Ferrara, A. M.; Botelho Do Rego, A. M. *Mater. Sci. Eng., C* **2006**, *26*, 253–259.
- (14) (a) He, T.; Corley, D. A.; Lu, M.; Di Spigna, N. H.; He, J.; Nackashi, D. P.; Franzon, P. D.; Tour, J. M. *J. Am. Chem. Soc.* **2009**, *131*, 10023–10030. (b) He, T.; Ding, H.; Peor, N.; Lu, M.; Corley, D. A.; Chen, B.; Ofir, Y.; Gao, Y.; Yitzchaik, S.; Tour, J. M. *J. Am. Chem. Soc.* **2008**, *130*, 1699–1710. (c) He, T.; He, J.; Lu, M.; Chen, B.; Pang, H.; Reus, W. F.; Nolte, W. M.; Nackashi, D. P.; Franzon, P. D.; Tour, J. M. *J. Am. Chem. Soc.* **2006**, *128*, 14537–14541.
- (15) Shalev, G.; Doron, A.; Virobnik, U.; Cohen, A.; Sanhedrai, Y.; Levy, I. *Appl. Phys. Lett.* **2008**, *93*, 083902.
- (16) Goykhman, I.; Korbakov, N.; Bartic, C.; Borghs, G.; Spira, M. E.; Shappir, J.; Yitzchaik, S. *J. Am. Chem. Soc.* **2009**, *131*, 4788–4794.
- (17) (a) Kang, B. S.; Ren, F.; Wang, L.; Lofton, C.; Tan, W. W.; Pearton, S. J.; Dabiran, A.; Osinsky, A.; Chow, P. P. *Appl. Phys. Lett.* **2005**, *87*, 023508. (b) Kang, B. S.; Wang, H. T.; Ren, F.; Pearton, S. J. *J. Appl. Phys.* **2008**, *104*, 031101.
- (18) Song, J.; Lu, W. *Appl. Phys. Lett.* **2006**, *89*, 223503.
- (19) Kokawa, T.; Sato, T.; Hasegawa, H.; Hashizume, T. *J. Vac. Sci. Technol. B* **2006**, *24*, 1972–1976.
- (20) Torsi, L.; Farinola, G. M.; Marinelli, F.; Tanese, M. C.; Omar, O. H.; Valli, L.; Babudri, F.; Palmisano, F.; Zambonin, P. G.; Naso, F. *Nat. Mater.* **2008**, *7*, 412–417.
- (21) Natan, A.; Kronik, L.; Haick, H.; Tung, R. T. *Adv. Mater.* **2007**, *19*, 4103–4117.
- (22) (a) Cohen, R.; Kronik, L.; Shanzer, A.; Cahen, D.; Liu, A.; Rosenwaks, Y.; Lorenz, J.; Ellis, A. B. *J. Am. Chem. Soc.* **1999**, *121*, 10545–10553. (b) Cohen, R.; Kronik, L.; Vilan, A.; Shanzer, A.; Rosenwaks, Y.; Cahen, D. *Adv. Mater.* **2000**, *12*, 33–37.
- (23) Kronik, L.; Shapira, Y. *Surf. Sci. Rep.* **1999**, *37*, 1–206.
- (24) (a) Shaya, O.; Shaked, M.; Doron, A.; Cohen, A.; Levy, I.; Rosenwaks, Y. *Appl. Phys. Lett.* **2008**, *93*, 043509. (b) Shaya, O.; Shaked, M.; Usherenko, Y.; Halpern, E.; Shalev, G.; Doron, A.; Levy, I.; Rosenwaks, Y. *J. Phys. Chem. C* **2009**, *113*, 6163–6168.
- (25) Shaya, O.; Amit, I.; Rosenwaks, Y. Unpublished work.
- (26) Devices based on nanowire or nanotube FETs may yet involve additional mechanisms, which are outside the scope of this article. For details see, for example: (a) Chen, R. J.; Choi, H. C.; Bangsaruntip, S.; Yenilmez, E.; Tang, X.; Wang, Q.; Chang, Y.-L.; Dai, H. *J. Am. Chem. Soc.* **2004**, *126*, 1563–1568. (b) Khanal, D. R.; Wu, J. *Nano Lett.* **2007**, *7*, 2778–2783. (c) Peng, N.; Zhang, Q.; Chow, C. L.; Tan, O. K.; Marzari, N. *Nano Lett.* **2009**, *9*, 1626–1630.
- (27) Artzi, R.; Daube, S. S.; Cohen, H.; Naaman, R. *Langmuir* **2003**, *19*, 7392–7398.
- (28) Aqua, T.; Cohen, H.; Vilan, A.; Naaman, R. *J. Phys. Chem. C* **2007**, *111*, 16313–16318.
- (29) *Handbook of Chemistry and Physics*, 84th ed.; Lide, D. R., Ed.; CRC Press LLC: Boca Raton, FL, 2004.
- (30) Morawski, A.; Slusarczuk, M. M. G.; Lagowski, J.; Gatos, H. C. *Surf. Sci.* **1977**, *69*, 53.
- (31) Shpaysman, H.; Salomon, E.; Neshet, G.; Vilan, A.; Cohen, H.; Kahn, A.; Cahen, D. *J. Phys. Chem. C* **2009**, *113*, 3313–3321.
- (32) Chang, G. S.; Hwang, W. C.; Wang, Y. C.; Yang, Z. P.; Hwang, J. S. *J. Appl. Phys.* **1999**, *86*, 1765.
- (33) Lee, K.; Lu, G.; Facchetti, A.; Janes, D. B.; Marks, T. J. *Appl. Phys. Lett.* **2008**, *92*, 123509.
- (34) Non-negligible interaction across saturated hydrocarbon bridges has also been noted in other contexts. See, for example: Shephard, M. J.; Paddon-Row, M. N.; Jordan, K. D. *Chem. Phys.* **1993**, *176*, 289–304.
- (35) Kronik, L.; Leibovitch, M.; Fefer, E.; Korobov, V.; Shapira, Y. *J. Electron. Mater.* **1995**, *24*, 893–901.

AM9005622